

# UC San Diego

## UC San Diego Previously Published Works

### Title

Highly Stable Battery Pack via Insulated, Reinforced, Buckling-Enabled Interconnect Array

### Permalink

<https://escholarship.org/uc/item/599859c5>

### Journal

Small, 14(43)

### ISSN

1613-6810

### Authors

Yin, Lu  
Seo, Joon Kyo  
Kurniawan, Jonas  
[et al.](#)

### Publication Date

2018-10-01

### DOI

10.1002/sml.201800938

Peer reviewed

# Highly Stable Battery Pack via Insulated, Reinforced, Buckling-Enabled Interconnect Array

Lu Yin, Joon Kyo Seo, Jonas Kurniawan, Rajan Kumar, Jian Lv, Lingye Xie, Xinyu Liu, Sheng Xu,\* Ying S. Meng,\* and Joseph Wang\*

This work describes a flexible and stretchable battery pack configuration that exhibits highly stable performance under large deformation up to 100% biaxial stretching. Using stress-enduring printable inks and serpentine interconnects, the new screen-printing route offers an attractive solution for converting rigid battery units into a flexible, stretchable energy storage device. Coin-cell lithium ion batteries are thus assembled onto the island regions of a screen-printed, buckling-enabled, polymer-reinforced interconnect “island-bridge” array. Most of the strain on the new energy-storage device is thus accommodated by the stress-enduring serpentine structures, and the array is further reinforced by mechanically strong “backbone” layers. Battery pack arrays are assembled and tested under different deformation levels, demonstrating a highly stable performance (<2.5% change) under all test conditions. A light emitting diode band powered by the battery pack is tested on-body, showing uninterrupted illumination regardless of any degrees of deformation. Moreover, battery-powered devices that are ultrastable under large deformation can be easily fabricated by incorporating different electronics parts such as sensors or integrated circuits on the same platform. Such ability to apply traditionally rigid, bulky lithium ion batteries onto flexible and stretchable printed surfaces holds considerable promise for diverse wearable applications.

In the past decades, the field of wearable electronics has been experiencing significant advances. Technology has been integrated into almost everything we touch, hear, wear, and see.<sup>[1–9]</sup> One of the major driving forces to this boom was the concept of “internet of things,” where hundreds of devices consume data and decipher new patterns in a single, connected network.<sup>[10]</sup> With the recent innovations in engineering and nanomaterials, the traditional, heavy, rigid, and bulky electronics have become miniature, thin, lightweight, flexible, stretchable, self-healing, or even disappear on demand.<sup>[11–28]</sup> Technology that was once thought to be impossible is thus becoming the new daily norm. As conformal electronics continue to embed themselves into every aspect of our lives, they demand less of our attention and

become invisible to common awareness or “unwearable.”<sup>[10,29–33]</sup> Unfortunately, this vision is currently constrained by bulky, low-density energy storage devices that prevent machines from seamlessly integrating into the human environment.<sup>[27]</sup> Realizing this vision requires also addressing concerns regarding the conformity and performance of energy storage devices under mechanical deformations caused by body movements.<sup>[34–37]</sup>

Among the different types of batteries, lithium ion batteries (LIBs) have been essential to the successful proliferation of electronic devices owing to their high energy density, power density, cycle life, and low cost.<sup>[27]</sup> The ability to apply traditionally rigid, bulky LIBs onto flexible surfaces will be critical to the success of conformal electronics. Efforts have thus been made to address this challenge, and stretchable batteries emphasizing on either the material or structural engineering approach were developed.<sup>[27]</sup> The material engineering approach focuses

on the modification on the battery material itself, where elastic polymers or high-aspect ratio conductive elements have been added into the battery, leading to conformal batteries capable of maintaining relatively stable electrochemical performance when deformation is applied.<sup>[8,38,39]</sup> However, such approach may suffer from erratic electrical performance (e.g., internal resistance, power output, columbic efficiency) with increasing the amount of strain applied to the structure.<sup>[40]</sup> On the other hand, the structural engineering approach commonly relies on ingenious design patterns where large strain can be successfully accommodated. Among all the efforts, island-bridge structures, commonly used in stretchable electronics, have been frequently adopted. In this approach, rigid functional components have been connected by serpentine structures that can buckle when stretched, thus achieving macroscale stretchability while retaining the shape and performance of individual functional components. Inspired by stretchable textiles, fiber-based batteries have also been demonstrated, where batteries are embedded into a yarn-shaped structure and can be further woven into stretchable clothes.<sup>[41,42]</sup> Similarly, inspirations from origami or kirigami have also led to intricate battery assemblies that are foldable and flexible.<sup>[43,44]</sup> Other approaches relying on the microstructures of the substrates (e.g., wrinkles or textile

L. Yin, Dr. J. K. Seo, J. Kurniawan, R. Kumar, J. Lv, L. Xie, X. Liu, Prof. S. Xu, Prof. Y. S. Meng, Prof. J. Wang  
Department of Nanoengineering  
University of California San Diego  
9500 Gilman Dr, La Jolla, CA 92093, USA  
E-mail: shengxu@ucsd.edu; shmeng@ucsd.edu; josephwang@ucsd.edu

 The ORCID identification number(s) for the author(s) of this article can be found under <https://doi.org/10.1002/sml.201800938>.

DOI: 10.1002/sml.201800938

embedded) have also demonstrated appreciable performance in flexibility and stretchability.<sup>[45,46]</sup> Yet, these mechanically engineered approaches usually include complex fabrication processes and intricate designs, and are thus low-throughput, presenting challenges of seamless integration of electronics onto the body.

Herein, we present a battery pack assembly that is durable under large strain while maintaining stable voltage and current output and nearly 100% columbic efficiency based on screen-printed interconnect arrays. The new stretchable battery pack adopts rigid coin-cell LIBs without the concern of failure, by relying the printed island-bridge array where strain is accommodated by the stress-enduring serpentine structures. With the resolution down to 50–100  $\mu\text{m}$ , screen-printing—a widely adopted thick-film fabrication process—is low-cost, high-throughput, and suitable for both prototyping and large-scale manufacturing of flexible and stretchable electronics.<sup>[8,9,47,48]</sup> Screen-printing can offer a wide range of complex patterns and intricate features based on various carbonaceous, metallic, or polymeric composite inks. Tailored for screen-printing, a formulated silver flexible ink is used here to construct a flexible conductive network along with a water-soluble ink for defining the free-standing region and enabling out-of-plane buckling during stretching while retaining the original low resistance.<sup>[19,49–51]</sup> A soft insulating polymer was printed on both sides of the free-standing serpentine to avoid any short-circuiting inside the battery pack. Further introduction of the proposed “backbone” layer via printing a mechanically strong polymer resin adds to the stability of the circuit, where the shape of the bonded region is protected from deformation, hence reducing the resistance changes due to expansion. Such novel all-printed island-bridge array offers high stability under deformation up to 100% biaxial stretching. The flexible energy-storage device is realized by fixing (and pressing) multiple LIBs onto the printed island containing a conductive paste. Dynamic voltage and current measurements and charging cycling tests under deformation of the assembled battery pack all give the stable performance with the relative change that is smaller than 2.5%, hence proving the successful integration of commercial LIBs with the novel printed interconnects. Therefore, a rigid commercial battery can be made into assemblies that are conformal, flexible, stretchable, making it thus suitable for energy applications that expect large deformation while maintaining a stable output.

The new stretchable battery pack relies on assembling commercially available coin-cell LIBs onto printed islands interconnected with free-standing stretchable serpentine bridges. The printing of the stretchable free-standing interconnect and the assembling process of the stretchable battery pack are illustrated in **Figure 1**. The ink is applied onto a metal stencil with designed patterns, and a squeegee is used to push the ink across the stencil to deposit ink, as shown in **Figure 1a**. This method is repeated for different layers, and the printing steps were summarized in **Figure 1b**. The backbone layer followed by the conductive flexible layer of the island region is firstly printed. Due to the extreme out-of-plane buckling that may take place during stretching, the conductive layer should have commensurate flexibility and conductivity to minimize change in resistance ( $\approx 1 \Omega$ ) and avoid the formation of permanent

damage. Here, an ink formulation, coupling silver flakes and an elastomer binder (Ag-SIS), described in our previous work,<sup>[52]</sup> is chosen owing to its superior flexibility and conductivity. Then, the water-soluble ink is printed to define the free-standing region of the interconnect. After curing, the insulation, conductive materials, followed by a second layer of insulation are printed sequentially on top of the cured water-soluble ink. The serpentine line-width is increased for insulation layers to ensure the complete encapsulation of the conductive layer and avoid short-circuiting during buckling. Lastly, a backbone layer is added on top of the serpentine connections for structural reinforcement. When preparing for the battery packs, the sacrificial layer is dissolved to allow serpentine to delaminate from the substrate and free to buckle upon stretching. The printed interconnect array before and after removing the sacrificial layer is shown in **Figure 1c,d**. The assembly of the stretchable battery pack is illustrated in **Figure 1e**. Seven Li-ion coin cell batteries were fixed under pressure in between two printed interconnects using an anisotropic conductive paste (ACP) that is printed onto the island regions. The ACP only forms conductive pathway along the direction of the pressure, hence avoiding any short circuiting in other directions. The assembled battery pack is demonstrated in **Figure 1f**. The substrate for the top contact array is chosen as a transparent PU sheet for the ease of demonstration. Using the method described above, the assembled battery packs is able to provide the stable voltage and current outputs, given rise to the novel backbone-reinforced, buckling-enabled, and insulated interconnect array.

The performance of the interconnect array is first studied. In comparison, a directly printed array, a printed buckling-enabled array without backbone support, and a buckling-enabled array with the backbone support are used. The stability of all three printed interconnect arrays is analyzed by measuring the resistance across the array during controlled stretching. Three printed arrays are stretched to 30%, 50%, and 100%, and the resistance measurement results are shown in **Figure 2a–c**, respectively. The directly printed array without any sacrificial layer is inherently bonded to the substrate and deforms with the substrate when external stress is applied. As the substrate stretches, the bonded island-bridge array expanded along the directions being stretched and demonstrated dramatic resistance change (plotted in black,  $>100 \Omega$  for 30% stretch,  $>10 \text{ k}\Omega$  for 50% and 100% stretch). This behavior is within expectation as the expansion further dispersed the finite number of conductive particles within the region. Hence, the direct-print method is evidently unsuitable for integration with the flexible and stretchable battery where large deformation is expected. On the other hand, the printed array with free-standing serpentine features showed a considerable increase in performance, where the resistance remained steadier compared to the bonded array (plotted in blue,  $<6 \Omega$  for 30% stretch and  $<1 \text{ k}\Omega$  for 50% stretch). However, the performance is not yet to be considered ideal for several reasons. Firstly, as iterations progress, the resistance increased incrementally throughout **Figure 2a–c**. Second, the change in resistance is still to be considered significant for interconnections of battery packs. High resistance inside the battery pack is undesired for both its negative effect on charging columbic efficiency and resistive heating that may damage the batteries and users when high current is

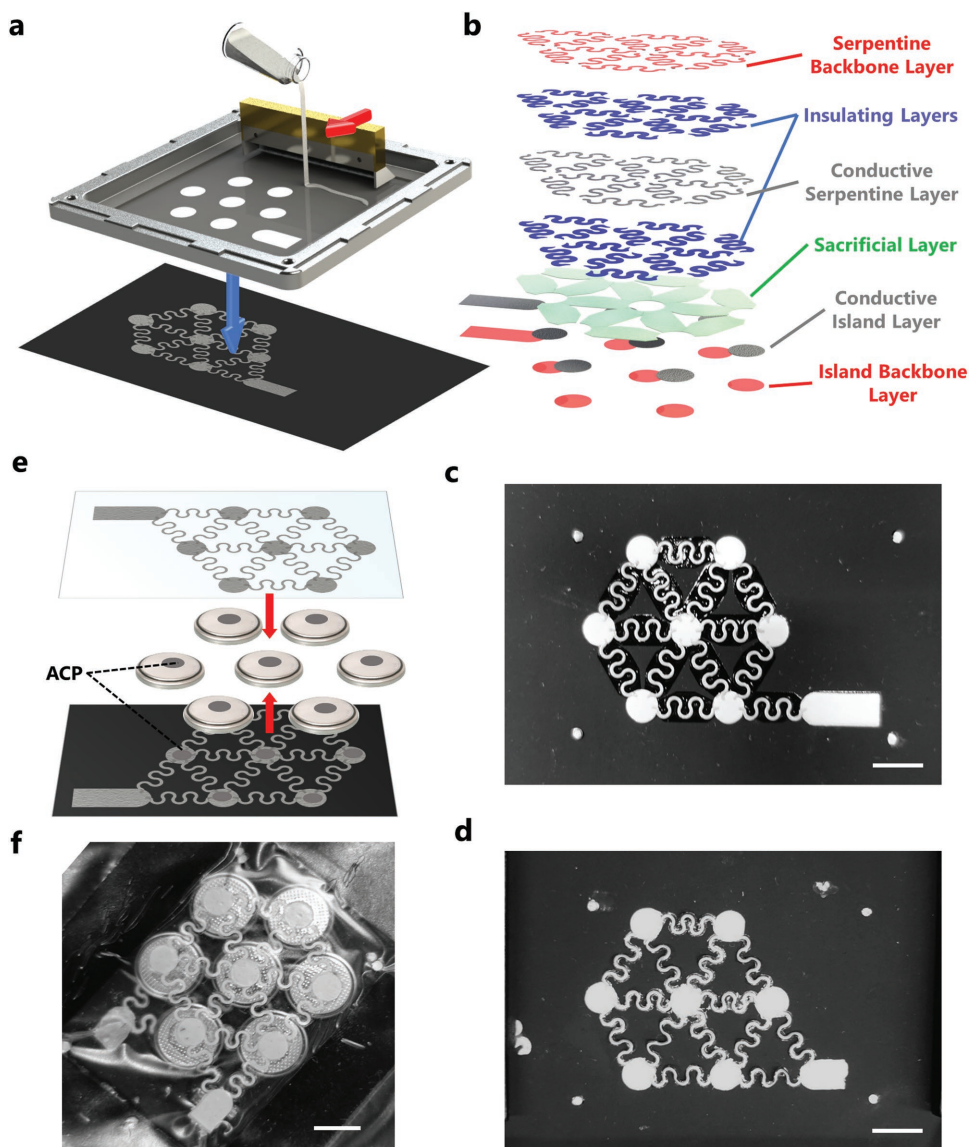


**Figure 1.** Fabrication process of printing free-standing island-bridge array with “backbone” and battery pack assembly. a) Schematics of the screen printing process. b) Structural illustration of the printed island-bridge array on the PU-laminated textile substrate. c) Printed array before dissolving the sacrificial layer on the PU-laminated textile substrate. d) Printed array after removing the sacrificial layer. e) Assembly of the printed array and Li-ion coin cell batteries using ACP as adhesive. f) Real image of assembled stretchable battery pack. Scale bar: 1 cm.

implemented. Third, as shown in the zoom-in view in Figure 2e (row 2, column 4), the island regions still expand with the substrate during stretching, which is similar to the behavior of the bonded array (row 1, column 4). This does not only contribute to the circuit resistance increase but also may cause delamination of the ACP that bonds batteries to the interconnect array.

In comparison, the printed free-standing array with backbone layer demonstrated superior mechanical performance, where the resistance remained to be less than  $5 \Omega$  for all 30%, 50%, and 100% stretch (plotted in red). It also showed the minimal incremental increase in resistance during a 100-cycle 100% stretch, presented in Figure 2d, indicating little fatigue effect on such printed compound structure. The 100% stretching repetition is demonstrated in Video S1 of the Supporting

Information, where the void of deformation on the island region and the reversible buckling of serpentine structures can be observed. A zoom-in view also demonstrated the stability introduced by the skeleton layer, where the island regions show little expansion when the substrate is stretched. The elimination of expansion leads to appreciably stable resistance during stretching, which will consequently benefit the performance of battery pack in reducing the internal resistance and increasing the columbic efficiency. In addition, as illustrated in the zoom-in view of column 5 in Figure 2e, by introducing backbone layer to the serpentine structures, the reinforced buckled serpentine structures (row 3) are able to retain its original serpentine structure after releasing the stress compared to the serpentine structures without the backbone reinforcement (row 2). The serpentine structures without

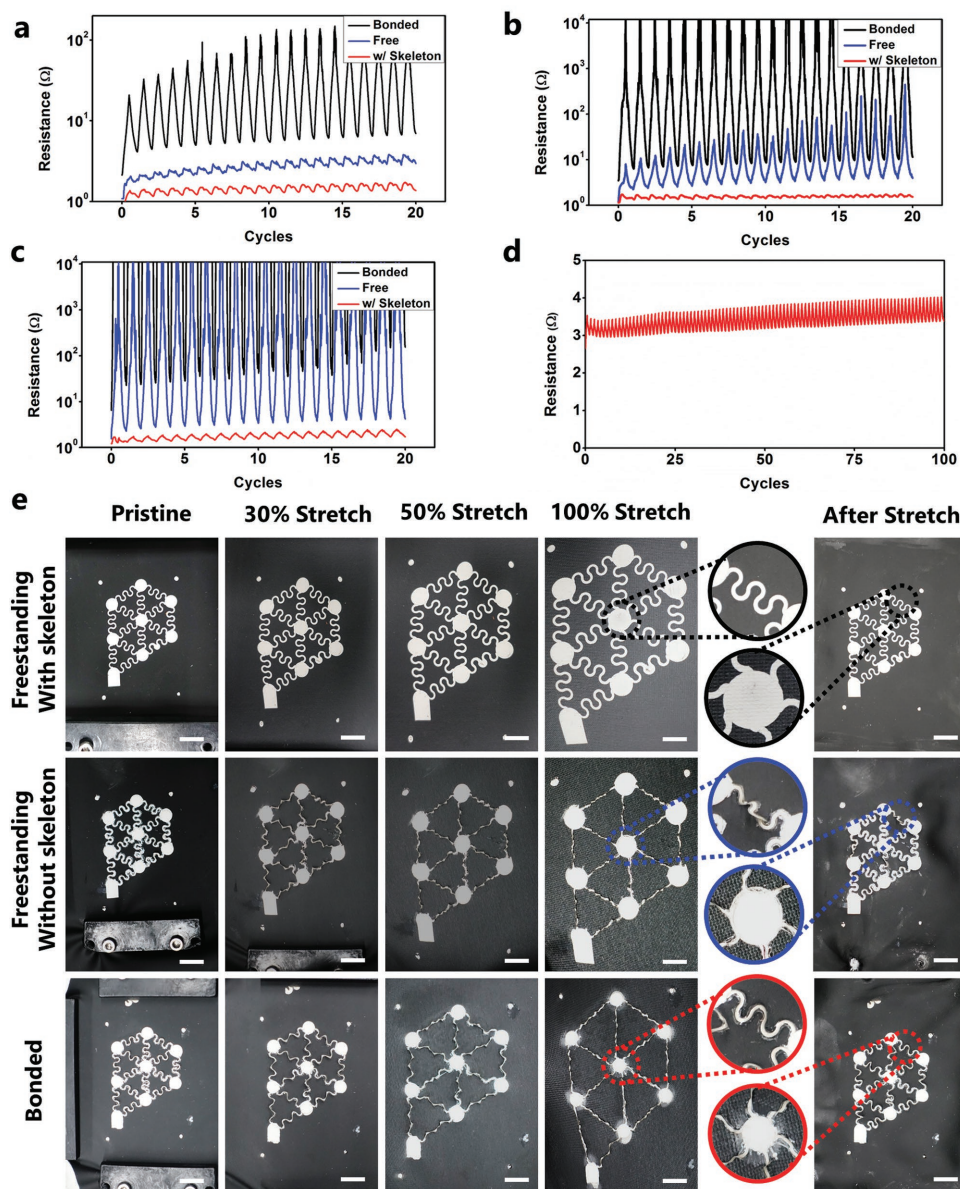


**Figure 2.** Comparison of bonded, free-standing, and free-standing with backbone island-bridge array. Conductivity measurement of bonded (black), free-standing without backbone (blue), and free-standing with backbone (red) during ten iterations of a) 30% stretch, b) 50% stretch, and c) 100% stretch. d) 100 cycles of 100% stretch of the free-standing island-bridge array with the backbone layer. e) Real images of free-standing array with the backbone (1st row), without the backbone layer (2nd row), and bonded array (3rd row) at 0% (1st column), 30% (2nd column), 50% (3rd column), 100% stretch (4th column), and after stretching (5th column), with zoom-in view of the island regions at 100% stretch. Scale bar: 1 cm.

reinforcement have shown some degree of entanglement after the large-strain stretching. This may be of concern when the entanglement of serpentine leads to the decrease in flexibility and stretchability. The printed interconnection array with free-standing serpentine and backbone layer reinforcement has shown a stable performance under different degrees of deformation and thus is considered as attractive configuration of interconnection for the stretchable battery pack.

Complemented by the resistivity study of the interconnect array, the mechanical and electrical performance of the assembled battery pack has been further studied by the measurement of voltage and current output under a fixed load, and

charge–discharge cycling during deformation. Here, battery packs assembled using the method above are connected to a 10 k $\Omega$  resistor and red light emitting diodes (LEDs) (as an indicator of circuit connection). An electrical measurement was carried out while controlled stretching iterations were implemented. The voltage across the load as well as the current through the circuit was measured during iterations of 10 cycles of 30%, 50%, and 100% stretch (Figure 3a–c). The battery packs demonstrate stable voltage and current outputs at all levels of large-strain deformation, which indicates a successful integration of individual batteries into a flexible, stretchable pack due to the superior mechanical performance of the printed interconnect

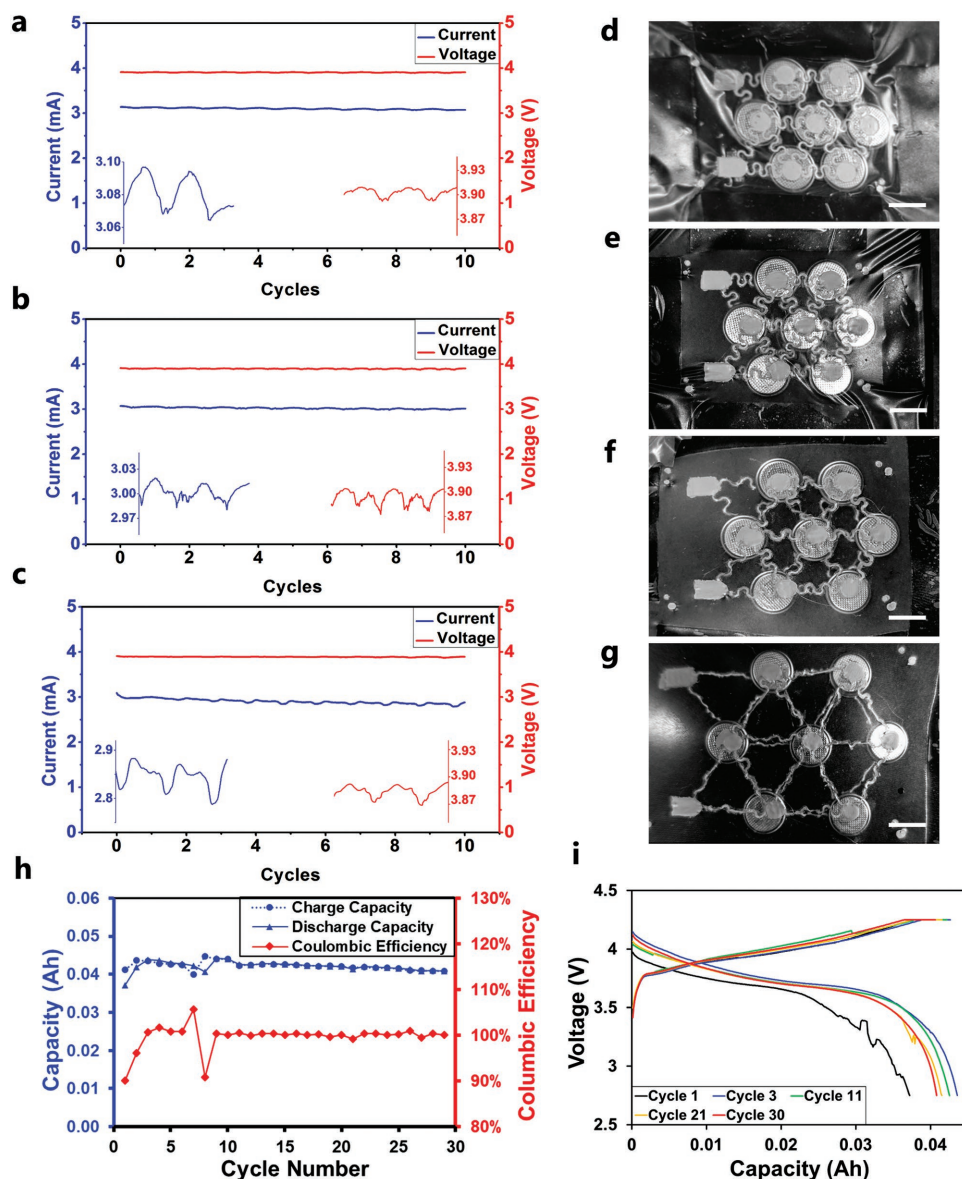


**Figure 3.** Battery array performance measurements. The open-circuit voltage and current under load during 10 cycles of a) 30%, b) 50%, and c) 100% stretch and the real image of the battery pack at d) 0% e) 30%, and f) 50% stretch, and g) 100% stretch. h) The C/10 charge/discharge capacity and corresponding coulombic efficiency while the battery pack is stretched to 0% (cycle 1–10), 30% (cycle 11–20), and 50% (cycle 21–30). i) The charge/discharge voltage profile at cycle 1, 3, 11, 21, and 30. Scale bar: 1 cm.

array. Zoom-in view of the measurement showed the periodic fluctuation of current ( $\pm 15 \mu\text{A}$  for 30% stretch,  $\pm 25 \mu\text{A}$  for 50% stretch, and  $\pm 35 \mu\text{A}$  for 100% stretch) and voltage ( $\pm 10 \text{ mV}$  for 30%, 50%, and 100% stretch), and is all within 2.5% of the average value. The long-term effect of stretching to the performance of the battery pack is also analyzed. The battery pack has undergone 30 charging cycles consecutively under 10/C c-rate while the entire pack is stretched to 0%, 30%, and 50%, with 10 cycles each, respectively (Figure 3h). The baseline is set at cycle 3 after several formation cycles, and the data from cycle 11, 21, and 30 are used as the comparison. The capacity of the battery pack remained constant during cycle 11–20 and 21–30, with nearly 100% coulombic efficiency, which indicates the low

internal resistance of the assembled battery pack even during long-term deformations. It is to be noted that the voltage profile showed constant decrease in discharge capacity after first few formation cycles, which may indicate the decrease in capacity is mainly contributed by the performance degradation of the coin cell batteries. The performance of the entire assembled flexible stretchable battery pack is overall stable and is free from loss in all the aspects of current output, voltage drop, or short-circuiting, as a result of the proposed buckling-enabled, backbone-reinforced, and insulated interconnect array.

Figure 4a suggests several possible locations where the battery pack can be placed. Due to the high mechanical stability of the battery pack exhibits, the placement of battery pack will

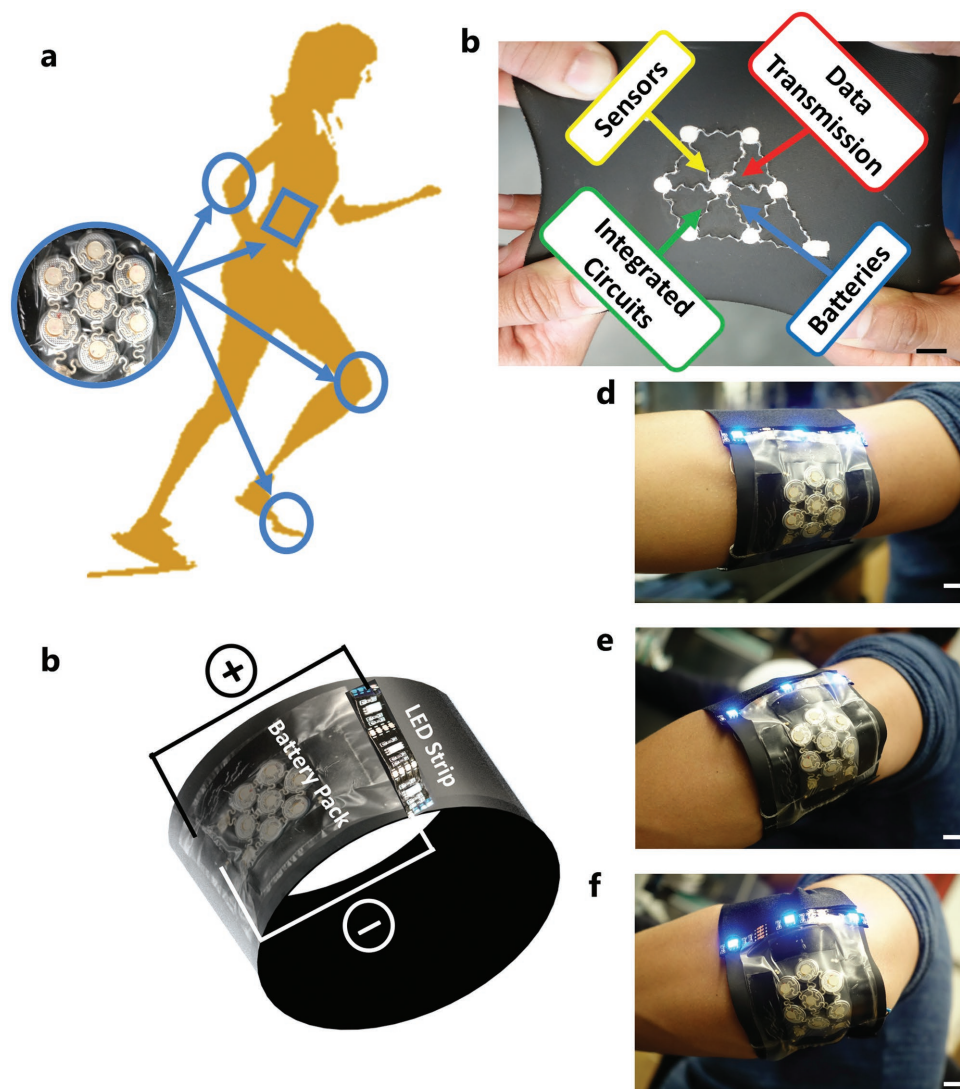


**Figure 4.** Battery pack on-body test and potential applications of free-standing island-bridge configurations. a) Illustration of suitable battery pack placement location. b) Illustration of using island-bridge configuration as a potential platform for integrating nonstretchable electronics into a conformal wearable device. c) The schematics of the assembly of a battery-pack-powered LED band. d–f) Assembled LED band on body at different deformation status. Scale bar: 1 cm.

no longer be limited to locations with little deformation. The battery pack can be integrated seamlessly with sportswear such as wrist bands, elbow, and knee protectors, running shoes or clothes with high conformity to human body, empowering a wide range of electronics for various applications. Moreover, the use of the presented all-printed island-bridge configuration is not limited to batteries but the entirety of electronic devices. Miniaturized electronics such as sensors, data transmission device, and integrated circuits can be incorporated onto the same island-bridge array powered by the batteries to become a wearable device that can endure large stretching deformation while maintaining optimal performance (Figure 4b). To put the assembled battery pack into use, an LED strip, the battery pack, and some stretchable conformal textiles are assembled into a wearable LED band, illustrated in Figure 4c. The LED band is placed to the user's elbow with the battery pack oriented on the

side with the most deformation. As Figure 4d–f and Video S2 (Supporting Information) show, the LED band has remained illuminated without interruption while the user exerts different levels of bending, suggesting the mechanical robustness and high stability of the stretchable flexible battery pack for large deformation applications.

In conclusion, we described an advanced printed interconnect array for assembling commercially available coin-cell LIBs as a conformal mechanically robust stretchable battery pack. Such flexible and stretchable battery pack has been realized using a novel screen-printed, buckling-enabled, backbone-reinforced, and insulated interconnection array implementing the island-bridge configuration. The addition of a water-soluble layer enabled the serpentine interconnects to be free-standing from the substrate and able to buckle when stress is applied to the battery pack. Further

modification on the array using a printable resin that gives a mechanically strong “backbone” significantly stabilized the resistance of printed array under the different degrees of deformation tested. When subjected to such external strain, the serpentine structures accommodate most of the stress, leaving the crucial coin-cell LIBs unharmed. The resistance of the printed array, the voltage, current, and charging efficiency have been analyzed under repetitive stretching. As a result, the resistance of the buckling-enabled array with the backbone layer has shown superior stability among other types; current and voltage output during stretching iterations and charge cycling data at different levels of deformation maintained appreciably stable. Using screen-printing, designated regions can be selectively insulated, exposed, free-standing, or bonded using a combination of screen-printable inks and printing steps, which other low-cost fabrication methods such as laser-cutting cannot offer. The printed interconnections with insulated free-standing serpentines and backbone-reinforcement offer an attractive solution for converting rigid battery units into a flexible, stretchable and stable energy storage device. The overall fabrication costs (materials and process) are extremely low compared to photolithography and laser-cutting, with most materials—except the silver flakes and Li-ion batteries—have negligible costs. Moreover, in a few steps, this solution can be applied to a more complex component configuration where circuits can be specially tailored for more intimate battery-electronics integration and enable biaxial stretchability and flexibility in a variety of wearable electronics. The successful adoption of such printed circuit architecture will enable the transition of various rigid electronics into conformal, flexible and stretchable electronics for the variety of wearable applications.

## Experimental Section

**Polymer Insulation Ink:** The polystyrene-*block*-polyisoprene-*block*-polystyrene (SIS) resin was prepared by dissolving the SIS beads (Aldrich, styrene 14 wt%) in toluene (6 g mL<sup>-1</sup>). The mixture was mixed using vortex machine overnight under room temperature.

**Ag-SIS Ink Formulation:** The conductive ink was prepared by mixing the silver flakes (Aldrich, 10 μm) with the SIS resin. The SIS resin (4 g mL<sup>-1</sup>) was prepared by dissolving the SIS beads (Aldrich, styrene 14 wt%) in toluene. The silver flakes were then mixed with the SIS resin with the weight ratio of 7:15 in a dual asymmetric centrifugal mixer (Flacktek Speedmixer, DAC 150.1 KV-K) at under the speed of 1800 rpm for 5 min. The ink was cured in room temperature for 10 min.

**Water Soluble Sacrificial Ink Formulation:** Pullulan (NutriScience Innovations, Trumbull, CT, USA) and Sucrose (C&H Professionals, Crockett, CA, USA) were used to formulate the sacrificial layer ink. The weight ratio of pullulan, sucrose, and water was optimized to be 2:2:5 to obtain the suitable viscosity for screen printing. The ink was cured for 10 min under 80 °C.

**Backbone Polymer Ink:** This commercial ink was purchased from Dupont Inc: 5036 Dielectric Paste (DuPont, Wilmington, DE, USA).

**Anisotropic Conductive Paste: The Assembling of Textile-Based Stretchable Battery Pack:** The commercial coin cell batteries were anchored on the printed interconnects using the anisotropic conductive paste (Creative Materials, Ayer, MA, USA). The ACP is composed of two parts: 124-19 Part A and CA-414 (Part B), which are mixed with a ratio of 100:22 (by weight) before applying. The ACP was precured for 5 min under 60 °C and was printed on the interconnects. Coin-cell batteries were placed cathodes facing the ACP on one of the arrays. Then another array with

printed ACP was attached to the anode side of the coin cells. The entire battery pack was then pressured using clamps for >6 h.

**Testing:** The volunteer subject was fully informed about the safety of the on-body testing procedure, and signed an appropriate consent.

## Supporting Information

Supporting Information is available from the Wiley Online Library or from the author.

## Acknowledgements

L.Y., J.K.S., J.K., and R.K. contributed equally to this work. This publication was supported by Advanced Research Projects Agency-Energy (DE-AR0000535) and the Defense Threat Reduction Agency Joint Science and Technology Office for Chemical and Biological Defense (HDTRA 1-16-1-0013). R.K. acknowledges the National Science Foundation Graduate Research Fellowship under Grant No. (DGE-1144086). Any opinion, findings, and conclusions or recommendations expressed in this material are those of the author(s) and do not necessarily reflect the views of the Department of Energy, DTRA, or National Science Foundation. J.L. acknowledges the support from the Scholarship Fund by China Scholarship Council (CSC).

## Conflict of Interest

The authors declare no conflict of interest.

## Keywords

island-bridge, screen-printing, stretchable, textile-based, wearable electronics

Received: March 9, 2018

Revised: April 5, 2018

Published online: July 3, 2018

- [1] T. Yamada, Y. Hayamizu, Y. Yamamoto, Y. Yomogida, A. Izadi-Najafabadi, D. N. Futaba, K. Hata, *Nat. Nanotechnol.* **2011**, *6*, 296.
- [2] R. K. Mishra, L. J. Hubble, A. Martín, R. Kumar, A. Barfidokht, J. Kim, M. M. Musameh, I. L. Kyratzis, J. Wang, *ACS Sens.* **2017**, *2*, 553.
- [3] J. J. Boland, *Nat. Mater.* **2010**, *9*, 790.
- [4] N. Cui, L. Gu, J. Liu, S. Bai, J. Qiu, J. Fu, X. Kou, H. Liu, Y. Qin, Z. L. Wang, *Nano Energy* **2015**, *15*, 321.
- [5] J. R. Sempionatto, T. Nakagawa, A. Pavinatto, S. T. Mensah, S. Imani, P. Mercier, J. Wang, *Lab Chip* **2017**, *17*, 1834.
- [6] M. Stoppa, A. Chiolerio, *Sensors* **2014**, *14*, 11957.
- [7] A. J. Bandothkar, I. Jeeran, J. Wang, *ACS Sens.* **2016**, *1*, 464.
- [8] J. Kim, R. Kumar, A. J. Bandothkar, J. Wang, *Adv. Electron. Mater.* **2017**, *3*, 1600260.
- [9] S. Shin, R. Kumar, J. W. Roh, D. S. Ko, H. S. Kim, S. Il Kim, L. Yin, S. M. Schlossberg, S. Cui, J. M. You, S. Kwon, J. Zheng, J. Wang, R. Chen, *Sci. Rep.* **2017**, *7*, 7317.
- [10] M. Weiser, *ACM SIGMOBILE Mobile Computing and Communications Review*, Vol. 3, ACM, NY **1999**, pp. 3–11.
- [11] S. Berchmans, A. J. Bandothkar, W. Jia, J. Ramírez, Y. S. Meng, J. Wang, *J. Mater. Chem. A* **2014**, *2*, 15788.
- [12] R. C. Webb, A. P. Bonifas, A. Behnaz, Y. Zhang, K. J. Yu, H. Cheng, M. Shi, Z. Bian, Z. Liu, Y.-S. Kim, W.-H. Yeo, J. S. Park, J. Song, Y. Li, Y. Huang, A. M. Gorbach, J. A. Rogers, *Nat. Mater.* **2013**, *12*, 938.

- [13] R. C. Webb, R. M. Pielak, P. Bastien, J. Ayers, J. Niittynen, J. Kurniawan, M. Manco, A. Lin, N. H. Cho, V. Malyrchuk, G. Balooch, J. A. Rogers, *PLoS One* **2015**, *10*, e0118131.
- [14] L. Tian, Y. Li, R. C. Webb, S. Krishnan, Z. Bian, J. Song, X. Ning, K. Crawford, J. Kurniawan, A. Bonifas, J. Ma, Y. Liu, X. Xie, J. Chen, Y. Liu, Z. Shi, T. Wu, R. Ning, D. Li, S. Sinha, D. G. Cahill, Y. Huang, J. A. Rogers, *Adv. Funct. Mater.* **2017**, *27*, 1701282.
- [15] S. Krishnan, Y. Shi, R. C. Webb, Y. Ma, P. Bastien, K. E. Crawford, A. Wang, X. Feng, M. Manco, J. Kurniawan, E. Tir, Y. Huang, G. Balooch, R. M. Pielak, J. A. Rogers, *Microsyst. Nanoeng.* **2017**, *3*, 17014.
- [16] R. C. Webb, Y. Ma, S. Krishnan, Y. Li, S. Yoon, X. Guo, X. Feng, Y. Shi, M. Seidel, N. H. Cho, J. Kurniawan, J. Ahad, N. Sheth, J. Kim, J. G. Taylor, T. Darlington, K. Chang, W. Huang, J. Ayers, A. Gruebele, R. M. Pielak, M. J. Slepian, Y. Huang, A. M. Gorbach, J. A. Rogers, *Sci. Adv.* **2015**, *1*, e1500701.
- [17] A. M. V. Mohan, N. Kim, Y. Gu, A. J. Bandodkar, J.-M. You, R. Kumar, J. F. Kurniawan, S. Xu, J. Wang, *Adv. Mater. Technol.* **2017**, *2*, 1600284.
- [18] A. J. Bandodkar, J.-M. You, N.-H. Kim, Y. Gu, R. Kumar, A. M. V. Mohan, J. Kurniawan, S. Imani, T. Nakagawa, B. Parish, M. Parthasarathy, P. P. Mercier, S. Xu, J. Wang, *Energy Environ. Sci.* **2017**, *10*, 1581.
- [19] S. Xu, Y. Zhang, J. Cho, J. Lee, X. Huang, L. Jia, J. A. Fan, Y. Su, J. Su, H. Zhang, H. Cheng, B. Lu, C. Yu, C. Chuang, T. Il Kim, T. Song, K. Shigeta, S. Kang, C. Dagdeviren, I. Petrov, P. V. Braun, Y. Huang, U. Paik, J. A. Rogers, *Nat. Commun.* **2013**, *4*, 1543.
- [20] C. Dagdeviren, Y. Su, P. Joe, R. Yona, Y. Liu, Y.-S. Kim, Y. Huang, A. R. Damadoran, J. Xia, L. W. Martin, Y. Huang, J. A. Rogers, *Nat. Commun.* **2014**, *5*, 4496.
- [21] A. J. Bandodkar, V. Mohan, C. S. López, J. Ramírez, J. Wang, *Adv. Electron. Mater.* **2015**, *1*, 1500289.
- [22] Q. Zhang, L. Liu, C. Pan, D. Li, *J. Mater. Sci.* **2018**, *53*, 27.
- [23] K. J. Yu, Z. Yan, M. Han, J. A. Rogers, *npj Flexible Electron.* **2017**, *1*, 4.
- [24] Y. Liu, M. Pharr, G. A. Salvatore, *ACS Nano* **2017**, *11*, 9614.
- [25] N. Matsuhisa, D. Inoue, P. Zalar, H. Jin, Y. Matsuba, A. Itoh, T. Yokota, D. Hashizume, T. Someya, *Nat. Mater.* **2017**, *16*, 834.
- [26] D. H. Kim, J. A. Rogers, *Adv. Mater.* **2008**, *20*, 4887.
- [27] W. Liu, M. S. Song, B. Kong, Y. Cui, *Adv. Mater.* **2017**, *29*, 1603436.
- [28] S. Yang, Y. C. Chen, L. Nicolini, P. Pasupathy, J. Sacks, B. Su, R. Yang, D. Sanchez, Y. F. Chang, P. Wang, D. Schnyer, D. Neikirk, N. Lu, *Adv. Mater.* **2015**, *27*, 6423.
- [29] I. Jeerapan, J. R. Sempionatto, A. Pavinatto, J.-M. You, J. Wang, *J. Mater. Chem. A* **2016**, *4*, 18342.
- [30] J. Kim, I. Jeerapan, S. Imani, T. N. Cho, A. Bandodkar, S. Cinti, P. P. Mercier, J. Wang, *ACS Sens.* **2016**, *1*, 1011.
- [31] A. Koh, D. Kang, Y. Xue, S. Lee, R. M. Pielak, J. Kim, T. Hwang, S. Min, A. Banks, P. Bastien, M. C. Manco, L. Wang, K. R. Ammann, K.-I. Jang, P. Won, S. Han, R. Ghaffari, U. Paik, M. J. Slepian, G. Balooch, Y. Huang, J. A. Rogers, *Sci. Transl. Med.* **2016**, *8*, 366ra165.
- [32] W. Gao, S. Emaminejad, H. Y. Y. Nyein, S. Challa, K. Chen, A. Peck, H. M. Fahad, H. Ota, H. Shiraki, D. Kiriya, D.-H. Lien, G. A. Brooks, R. W. Davis, A. Javey, *Nature* **2016**, *529*, 509.
- [33] T. Someya, T. Sekitani, S. Iba, Y. Kato, H. Kawaguchi, T. Sakurai, *Proc. Natl. Acad. Sci. USA* **2004**, *101*, 9966.
- [34] Y. Zhang, H. Fu, S. Xu, J. A. Fan, K. C. Hwang, J. Jiang, J. A. Rogers, Y. Huang, *J. Mech. Phys. Solids* **2014**, *72*, 115.
- [35] J. A. Fan, W. H. Yeo, Y. Su, Y. Hattori, W. Lee, S. Y. Jung, Y. Zhang, Z. Liu, H. Cheng, L. Falgout, M. Bajema, T. Coleman, D. Gregoire, R. J. Larsen, Y. Huang, J. A. Rogers, *Nat. Commun.* **2014**, *5*, 3266.
- [36] J. A. Rogers, T. Someya, Y. Huang, *Science* **2010**, *327*, 1603.
- [37] J. Viventi, D. H. Kim, J. D. Moss, Y. S. Kim, J. A. Blanco, N. Annetta, A. Hicks, J. Xiao, Y. Huang, D. J. Callans, J. A. Rogers, B. Litt, *Sci. Transl. Med.* **2010**, *2*, 24ra22.
- [38] A. J. Bandodkar, J.-M. You, N.-H. Kim, Y. Gu, R. Kumar, A. M. V. Mohan, J. Kurniawan, S. Imani, T. Nakagawa, B. Parish, M. Parthasarathy, P. P. Mercier, S. Xu, J. Wang, *Energy Environ. Sci.* **2017**, *10*, 1581.
- [39] S. Pang, Y. Gao, S. Choi, *Adv. Energy Mater.* **2018**, *8*, 1702261.
- [40] R. Kumar, J. Shin, L. Yin, J. M. You, Y. S. Meng, J. Wang, *Adv. Energy Mater.* **2017**, *7*, 1602096.
- [41] J. Ren, Y. Zhang, W. Bai, X. Chen, Z. Zhang, X. Fang, W. Weng, Y. Wang, H. Peng, *Angew. Chem.* **2014**, *126*, 7998.
- [42] Y. Xu, Y. Zhao, J. Ren, Y. Zhang, H. Peng, *Angew. Chem.* **2016**, *128*, 8111.
- [43] Z. Song, T. Ma, R. Tang, Q. Cheng, X. Wang, D. Krishnaraju, R. Panat, C. K. Chan, H. Yu, H. Jiang, *Nat. Commun.* **2014**, *5*, 3140.
- [44] Z. Song, X. Wang, C. Lv, Y. An, M. Liang, T. Ma, D. He, Y. J. Zheng, S. Q. Huang, H. Yu, H. Jiang, *Sci. Rep.* **2015**, *5*, 10988.
- [45] C. Wang, W. Zheng, Z. Yue, C. O. Too, G. G. Wallace, *Adv. Mater.* **2011**, *23*, 3580.
- [46] A. M. Gaikwad, A. M. Zamarayeva, J. Rousseau, H. Chu, I. Derin, D. A. Steingart, *Adv. Mater.* **2012**, *24*, 5071.
- [47] A. J. Bandodkar, I. Jeerapan, J. M. You, R. Nuñez-Flores, J. Wang, *Nano Lett.* **2016**, *16*, 721.
- [48] A. J. Bandodkar, R. Nuñez-Flores, W. Jia, J. Wang, *Adv. Mater.* **2015**, *27*, 3060.
- [49] S. Xu, Z. Yan, K.-I. Jang, W. Huang, H. Fu, J. Kim, Z. Wei, M. Flavin, J. McCracken, R. Wang, A. Badea, Y. Liu, D. Xiao, G. Zhou, J. Lee, H. U. Chung, H. Cheng, W. Ren, A. Banks, X. Li, U. Paik, R. G. Nuzzo, Y. Huang, Y. Zhang, J. A. Rogers, *Science* **2015**, *347*, 154.
- [50] Y. Zhang, S. Xu, H. Fu, J. Lee, J. Su, K.-C. Hwang, J. A. Rogers, Y. Huang, *Soft Matter* **2013**, *9*, 8062.
- [51] S. Xu, Y. Zhang, L. Jia, K. E. Mathewson, K. I. Jang, J. Kim, H. Fu, X. Huang, P. Chava, R. Wang, S. Bhole, L. Wang, Y. J. Na, Y. Guan, M. Flavin, Z. Han, Y. Huang, J. A. Rogers, *Science* **2014**, *344*, 70.
- [52] L. Yin, R. Kumar, A. Karajic, L. Xie, J. You, D. Joshua, C. S. Lopez, J. Miller, J. Wang, *Adv. Mater. Technol.* **2018**, 1800013.